IMPERIAL COLLEGE of SCIENCE, TECHNOLOGY & MEDICINE

DEPARTMENT of ELECTRICAL & ELECTRONIC ENGINEERING

MSc in Communications and Signal Processing

Formal Report No. 2

Name	Zhaolin Wang
Experiment Code	AM
Title of Experiment	Array Communications and Processing
Date of Submission	11/01/2021
Supervisor of Experiment	Dr. A. Manikas
Grade	

Communications, Control and Signal Processing Laboratory

Array Communications and Processing

Zhaolin Wang

Department of Electrical and Electronic Engineering
Imperial College London

Aims – Based on the experiment handout [1], simulate a theoretical framework for handling the various problems in the array communications, including the detection, estimation, and reception problem. This experiment emphasizes the "superresolution" approaches, which are robust to the noise in the channel.

NOMENCLATURE

$A,\ a$	Scalar
$\underline{A},\ \underline{a}$	Column vector
$\mathbf{A}$	Matrix
$\mathbf{1}_N$	Column vector of N ones
$\mathbf{I}_N$	N dimensional identity matrix
$(\cdot)^T$	Transpose
$(\cdot)^H$	Hermitian transpose
$\exp(\underline{a})$	Element-by-element exponential
$\mathbb{P}_A$	Projection operator on the space spanned by the column vectors of matrix A i.e., $\mathbb{P}_A = A(A^H A)^{-1}A^H$.
$\mathbb{P}_A^{\perp}$	Projection operator on the orthogonal space of the space spanned by the column vectors of matrix A i.e., $\mathbb{P}_A^{\perp} = I - \mathbb{P}_A$

I. INTRODUCTION

An array is formed by several receiving elements distributed in 3D Cartesian space. Based on the array, the information of the noisy communication environment consisting of a number of emitting sources can be obtained by the array processing techniques, where the emitting sources either reflect signals (passive antennas) or emit their own signals (active antennas). In the last several decades, a popular application of arrays is exploiting the space-time and not just time information in the digital communication systems. By integrating the array theory and digital communication theory, many new communication systems have been proposed, which have considerable impacts on

the performance and capacity of the mobile communication network.

In this experiment, the techniques addressing the three general problems (detection, estimation, and reception) for the array receiver in digital communication are investigated and simulated. The objective of the detection problem is to detect the number of co-channel emitting sources. Two cases are considered in the detection problem. The first case is that there are infinite observation snapshots of received signals, where the number of sources is estimated directly based on eigenvalues of signal covariance matrix, while the AIC or MDL criteria [2] can be used in this second case where there are finite snapshots. For the estimation problem, this experiment emphasis a superresolution approach called MuSIC algorithm [3], which can be used to estimate the directions of the sources. Based on the estimation result of the MuSIC algorithm, a superresolution beamformer, which is capable of receiving the desired signal and eliminating the co-channel interferences, is investigated in the reception problem. A comparison between this superresolution beamformer and conventional beamformer is also conducted in this experiment, which shows that the former is capable of eliminating the impact of noise on the resolution.

II. BACKGROUND

a) Array Manifold Vector [4]

There have been a large number of algorithms exploiting the structure of antenna arrays in the area of array processing and communication. All these algorithms are based on the concept of array manifold, which is the locus of the array manifold vectors. The array manifold vector is defined as

$$\underline{S}(\theta,\phi) = \exp\left(-j\left[\underline{r}_1, \underline{r}_2, \cdots, \underline{r}_N\right]^T \underline{k}(\theta,\phi)\right), \tag{1}$$

where $\left[\underline{r}_1, \underline{r}_2, \cdots, \underline{r}_N\right]^T$ is the location vectors of the N antennas in the 3-dimensional Cartesian coordinate system, θ is the azimuth angle, ϕ is the elevation angle, and $\underline{k}(\theta,\phi)$ is the wavenumber vector defined as

$$\underline{k}(\theta,\phi) = \frac{2\pi F_c}{c}\underline{u}(\theta,\phi) \tag{2}$$

$$\underline{u}(\theta,\phi) = [\cos\theta\cos\phi, \sin\theta\cos\phi, \sin\phi]^T \tag{3}$$

For equation (1), the plane wave propagation is assumed for the signals.

b) Array Pattern [4]

Array pattern provides the gain of the array in different directions which is defined as

$$g(\theta,\phi) = \underline{w}^H \underline{S}(\theta,\phi), \tag{4}$$

where $\underline{w}^H$ is the complex weights and $\underline{S}(\theta,\phi)$ is the array manifold vectors for the direction (θ,ϕ). When $\underline{w} = \underline{1}_N$, $g(\theta,\phi)$ is the default array pattern of an antenna array.

c) Multi-path SIMO Channel Modeling [4]

Assuming that there are L paths in a SIMO channel, the impulse response of the channel is

$$\underline{h}(t) = \sum_{\ell=1}^{L} \underline{S}(\theta_\ell,\phi_\ell)\cdot\beta_\ell\cdot\delta(t-\tau_\ell), \tag{5}$$

where (θ_ℓ,ϕ_ℓ) is the direction of the ℓ^{th} path arrives at the reference point of the antenna array, and β_ℓ and τ_ℓ are the channel fading coefficient and delay of the ℓ^{th} path, respectively.

Considering the signal $m(t)$ transmitted through the SIMO channel, the received signal can be modeled as

$$\underline{x}(t) = \underline{h}(t) * m(t) + \underline{n}(t) \tag{6a}$$

$$= \sum_{\ell=1}^{L} \underline{S}(\theta_\ell,\phi_\ell)\cdot\beta_\ell\cdot m(t-\tau_\ell) + \underline{n}(t) \tag{6b}$$

$$= \mathbf{S}\underline{m}(t) + \underline{n}(t) \tag{6c}$$

where

$$\mathbf{S} = \left[\underline{S}_1, \underline{S}_2, \cdots, \underline{S}_L\right], with\ \underline{S}_\ell \triangleq \underline{S}(\theta_\ell,\phi_\ell), \tag{7}$$

$$\underline{m}(t) = [\beta_1 m(t-\tau_1), \beta_2 m(t-\tau_2), \cdots \beta_L m(t-\tau_L)]^T, \tag{8}$$

and $\underline{n}(t)$ is the additive noise in the channel.

In the multi-user scenario with M users, the signal (6) can be further modeled as

$$\underline{x}(t) = \sum_{i=1}^{M}\sum_{\ell=1}^{L} \underline{S}(\theta_{i\ell},\phi_{i\ell})\cdot\beta_{i\ell}\cdot m_i(t-\tau_{i\ell}) + \underline{n}(t) \tag{9}$$

III. EXPERIMENT ON ARRAY COMMUNICATION AND PROCESSING

A linear array of 5 uniformly distributed sensors is used in this experiment. The locations of the linear array in 3-dimensional Cartesian coordinate system in unite of half-wavelength is

$$array = [\underline{r}_1, \underline{r}_2, \cdots, \underline{r}_5]^T = \begin{bmatrix} -2 & 0 & 0 \\ -1 & 0 & 0 \\ 0 & 0 & 0 \\ 1 & 0 & 0 \\ 2 & 0 & 0 \end{bmatrix}, \tag{10}$$

and the directions of the three received noisy signals in the same frequency band are $(30^\circ, 0^\circ)$, $(35^\circ, 0^\circ)$, and $(90^\circ, 0^\circ)$. The default array pattern of (10) calculated by (4) is shown below.

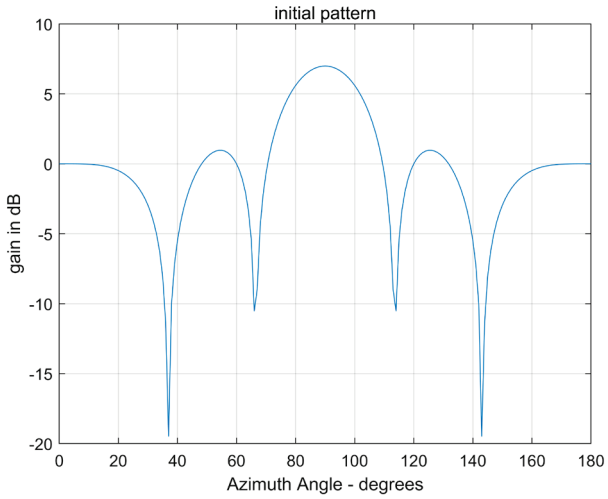

Fig. 1 Default array pattern of the array defined by (10)

Based on the second-order statistics, that is the covariance matrix $\mathbf{R}_{xx}$, the detection, estimation, and reception problems can be addressed. Three covariance matrices are considered in this experiment, including a theoretical one for three sources with equal power and two practical ones of three audio signals and three colour images, respectively.

According to equation (6) and (9), the theoretical covariance is given by

$$\mathbf{R}_{xx,theoretical} = \mathbb{E}[\underline{x}(t)\underline{x}(t)^H] = \mathbf{S} \cdot \mathbf{R}_{mm} \cdot \mathbf{S}^H + \sigma^2 \mathbf{I}_N \tag{11}$$

where $N = 5$ in this experiment, $\mathbf{S}$ is the array manifold vectors defined by the array locations (10) and the directions of three sources, σ^2 is the power of noise, and $\mathbf{R}_{mm}$ is the covariance matrix of the three sources. In the case where the three sources are uncorrelated and of equal power 1, $\mathbf{R}_{mm}$ is

$$\mathbf{R}_{mm} = \begin{bmatrix} \mathbb{E}[m_1(t)m_1(t)^*] & \mathbb{E}[m_1(t)m_2(t)^*] & \mathbb{E}[m_1(t)m_3(t)^*] \\ \mathbb{E}[m_2(t)m_1(t)^*] & \mathbb{E}[m_2(t)m_2(t)^*] & \mathbb{E}[m_2(t)m_3(t)^*] \\ \mathbb{E}[m_3(t)m_1(t)^*] & \mathbb{E}[m_3(t)m_2(t)^*] & \mathbb{E}[m_3(t)m_3(t)^*] \end{bmatrix} = \begin{bmatrix} 1 & 0 & 0 \\ 0 & 1 & 0 \\ 0 & 0 & 1 \end{bmatrix}, \tag{12}$$

while when there are two sources are fully correlated (i.e., the two sources in the directions $(30^\circ, 0^\circ)$, $(35^\circ, 0^\circ)$), the $\mathbf{R}_{mm}$ is

$$\mathbf{R}_{mm} = \begin{bmatrix} 1 & 1 & 0 \\ 1 & 1 & 0 \\ 0 & 0 & 1 \end{bmatrix}. \tag{13}$$

Both two cases are considered in the estimation problems.

In practice, infinite observation snapshots cannot be obtained, therefore the practical covariance can be estimated based on L finite snapshots using the following formula

$$\mathbf{R}_{xx,practical} = \frac{1}{L}\sum_{l=1}^{L} \underline{x}(t_l)\underline{x}(t_l)^H \tag{14}$$

where $\underline{x}(t_l)$ is a snapshot of the received signal sampled at the time t_l.

a) Detection Problem

The objective of the detection problem for the array receiver is detecting the number of co-channel emitting sources (denoted by M). Observing the expression of $\mathbf{R}_{xx,theoretical}$ in (11), it can be rewritten as

$$\mathbf{R}_{xx,theoretical} = \mathbf{R}_{signal} + \sigma^2\mathbf{I}_N \tag{15}$$

where $\mathbf{R}_{signal} = \mathbf{S}\cdot\mathbf{R}_{mm}\cdot\mathbf{S}^H$. As there are M emitting sources, the rank of $\mathbf{R}_{signal}$ is M, leading to M non-zeros eigenvalues of $\mathbf{R}_{signal}$. Therefore, using the eigen-decomposition of $\mathbf{R}_{signal}$,

$$\begin{aligned} \mathbf{R}_{xx,theoretical} &= \mathbf{E}\cdot\mathbf{\Lambda}\cdot\mathbf{E}^H + \sigma^2\mathbf{I}_N \\ &= \mathbf{E}\cdot(\mathbf{\Lambda} + \sigma^2\mathbf{I}_N)\cdot\mathbf{E}^H \end{aligned} \tag{16}$$

where $\mathbf{\Lambda}$ is an $N \times N$ diagonal matrix consisting of the eigenvalues of $\mathbf{R}_{signal}$, and

$$\mathbf{\Lambda} = \begin{bmatrix} \lambda_1 & 0 & \cdots & 0 & 0 & \cdots & 0 \\ 0 & \lambda_2 & \cdots & 0 & 0 & \cdots & 0 \\ \cdots & \cdots & \cdots & \cdots & \cdots & \cdots & \cdots \\ 0 & 0 & \cdots & \lambda_M & 0 & \cdots & 0 \\ 0 & 0 & \cdots & 0 & 0 & \cdots & 0 \\ \cdots & \cdots & \cdots & \cdots & \cdots & \cdots & \cdots \\ 0 & 0 & \cdots & 0 & 0 & \cdots & 0 \end{bmatrix} \tag{17}$$

The equation (16) can be regarded as the eigen-decomposition of $\mathbf{R}_{xx,theoretical}$, and the diagonal eigenvalue matrix of $\mathbf{R}_{xx,theoretical}$ is given as

$$\mathbf{D} = \mathbf{\Lambda} + \sigma^2\mathbf{I}_N = \begin{bmatrix} \lambda_1+\sigma^2 & 0 & \cdots & 0 & 0 & \cdots & 0 \\ 0 & \lambda_2+\sigma^2 & \cdots & 0 & 0 & \cdots & 0 \\ \cdots & \cdots & \cdots & \cdots & \cdots & \cdots & \cdots \\ 0 & 0 & \cdots & \lambda_M+\sigma^2 & 0 & \cdots & 0 \\ 0 & 0 & \cdots & 0 & \sigma^2 & \cdots & 0 \\ \cdots & \cdots & \cdots & \cdots & \cdots & \cdots & \cdots \\ 0 & 0 & \cdots & 0 & 0 & \cdots & \sigma^2 \end{bmatrix} \tag{18}$$

Remark 1. *In theory, the number of emitting sources can be estimated according to the eigenvalues of the covariance matrix using the following expression* $M = N - multiplicity\ of\ minimum\ eigenvalues\ of\ \mathbf{R}_{xx}$.

Remark 2. *The power of noise can be estimated by the average value of* $N - M$ *smallest values of eigenvalues of the covariance matrix of received signals.*

In this experiment, the $\mathbf{R}_{xx,theoretical}$ is implemented using the array locations (10) and covariance matrix $\mathbf{R}_{mm}$ in (12) with directions $(30^{\circ}, 0^{\circ})$, $(35^{\circ}, 0^{\circ})$, and $(90^{\circ}, 0^{\circ})$ as well as the noise power $\sigma^2 = 0.0001$. The eigenvalues of this $\mathbf{R}_{xx,theoretical}$ are

$$[9.9369, 4.9681, 0.0953, 0.0001, 0.0001], \tag{19}$$

where the last two eigenvalues equal to the noise power σ^2, which validates the **Remark 2**. The number of multiple minimum eigenvalues is 2, therefore the number of emitting sources can be estimated by $M = N - 2 = 5 - 2 = 3$, which validates **Remark 1**.

For the audio and image signals given in this experiment, the covariance matrix $\mathbf{R}_{xx,audio}$ and $\mathbf{R}_{xx,image}$ are estimated using formula (14). The eigenvalues of these two covariance matrices are calculated and the results are shown below.

$$audio\ signal: [4.328 \times 10^5, 1.072 \times 10^4, 1.733 \times 10^2, 0.0101, 0.0100] \tag{20}$$

$$image\ signal: [2.178 \times 10^5, 2.039 \times 10^4, 1.909 \times 10^2, 7.061 \times 10^{-11}, -9.492 \times 10^{-11}], \tag{21}$$

It is noticeable that the last two eigenvalues in both (20) and (21) are much smaller than the first three eigenvalues, therefore the last two eigenvalues represent the noise power of the signal and the number of emitting sources in audio and image signals can also estimate by $M = N - 2 = 5 - 2 = 3$.

However, this estimation method only suitable for the case where the SNR is high. The 250 snapshots of signals containing three emitting sources are simulated with different noise powers. In the case where SNR is 40dB, the eigenvalues are

$$[9.5108, 5.7729, 0.0849, 1.0406 \times 10^{-4}, 8.9192 \times 10^{-5}]. \tag{22}$$

Although the last two values in (22) are not identical, they are much smaller than the first three eigenvalues. Therefore, it is easy to observe that the number of emitting sources is $M = 3$ based on (22). In the case where SNR is 10dB, the eigenvalues are

$$[10.1437, 5.0479, 0.2216, 0.1038, 0.0902]. \tag{23}$$

In (23), it is difficult to determine the number of sources. Thus, a more powerful method called the information theoretic criteria [2], including Akaike Information Criterion (AIC) and Minimum Description Length (MDL), is usually used in practice. The number of emitting sources can be estimated by $M = \arg\min_k\{\mathrm{AIC}(k)\}$ or $M = \arg\min_k\{\mathrm{MDL}(k)\}$ $(k = 0,1 \cdots N-1)$. $\mathrm{AIC}(k)$ and $\mathrm{MDL}(k)$ are defined as

$$\mathrm{AIC}(k) = -2\ln\left(\frac{\prod_{\ell=k+1}^{N} d_l^{\frac{1}{N-k}}}{\frac{1}{N-k}\sum_{\ell=k+1}^{N} d_\ell}\right)^{(N-k)L} + 2k(2N-k) \tag{24}$$

$$\mathrm{MDL}(k) = -\ln\left(\frac{\prod_{\ell=k+1}^{N} d_l^{\frac{1}{N-k}}}{\frac{1}{N-k}\sum_{\ell=k+1}^{N} d_\ell}\right)^{(N-k)L} + \frac{1}{2}k(2N-k)\ln L \tag{25}$$

where d_ℓ is the ℓ^{th} eigenvalues of the covariance matrix $\mathbf{R}_{xx}$ sorted from the largest to the smallest, N is the number of antennas in the array, and L is the length of snapshots. Appling the AIC and MDL criteria in the case where the SNR is 10dB, the AIC and MDL vectors are

$$\mathrm{AIC} = [4098.3, 2997.4, 113.6, 43.6, 48.0] \tag{26}$$

$$\mathrm{MDL} = [2048.1, 1514.5, 85.0, 58.8, 66.3] \tag{27}$$

The fourth value in both (26) and (27) is the smallest one, which is related to $k = 3$. Therefore, both AIC and MDL get the correct estimation result $M = 3$ with relatively low SNR (i.e., 10dB). The correct results can also be obtained in the case where SNR is high (i.e., 40dB). Therefore, AIC and MDL criteria are capable of degrading the impact of noise on the resolution of detecting the number of emitting sources.

b) Estimation Problem

Another significant task for array receivers is to estimate various signal and channel parameters, such as direction of arrival (DOA), delay, and fading coefficient. This experiment concentrates on the estimation of DOAs of the sources using a superresolution approach – MuSIC algorithm [3]. Based on the orthogonality between then signal space and the noise space in (6), the MuSIC cost function is defined as

$$\xi(p) = \frac{1}{\underline{S}(p)^H \cdot \mathbb{P}_{\mathbf{E}_n} \cdot \underline{S}(p)} \tag{28}$$

where $\underline{S}(p)$ is the array manifold vector with parameter p (p is the azimuth angle θ in this experiment), and $\mathbb{P}_{\mathbf{E}_n}$

is the project matrix of the noise space. For the estimated unknown parameter p, $\underline{S}(p)^H \cdot \mathbb{P}_{\mathbf{E}_n} \cdot \underline{S}(p) = 0$. Therefore, by searching all the possible p, the desired ones can be obtained when the $\xi(p)$ is large enough.

For the theoretical covariance matrix implemented using the uncorrelated $\mathbf{R}_{mm}$ in (12) with the DOAs of $(30^\circ, 0^\circ)$, $(35^\circ, 0^\circ)$, and $(90^\circ, 0^\circ)$, the number of emitting sources is $M = 3$. Thus, the eigenvectors of the noise space $\mathbf{E}_n$ are the two vectors corresponding to the two smallest eigenvalues of the covariance matrix. Then the MuSIC spectrum can be plotted by calculating the $\xi(p)$ for all parameter p, which is shown in Fig. 2. In Fig. 2, there are three obvious large gains at the azimuth of 30°, 35°, and 90°.

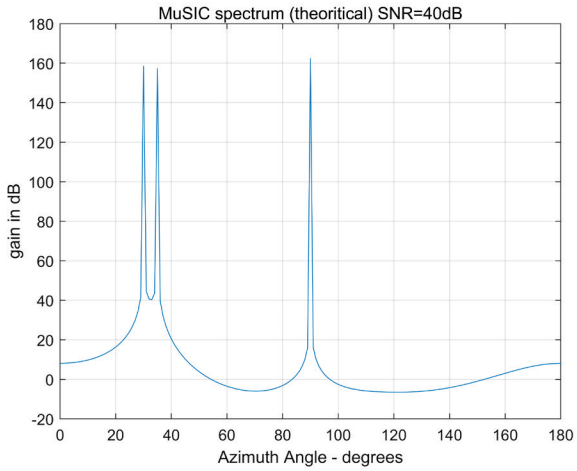

Fig. 2 MuSIC spectrum of the theoretical covariance matrix

For the covariance matrices of the audio signal and image signal, the number of emitting sources is detected using AIC or MDL method before applying the MuSIC algorithm. The similar MuSIC spectrums are obtained, which are shown in Fig. 3. According to the MuSIC spectrums, both two signals have the sources arriving in the directions of $(30^\circ, 0^\circ)$, $(35^\circ, 0^\circ)$, and $(90^\circ, 0^\circ)$.

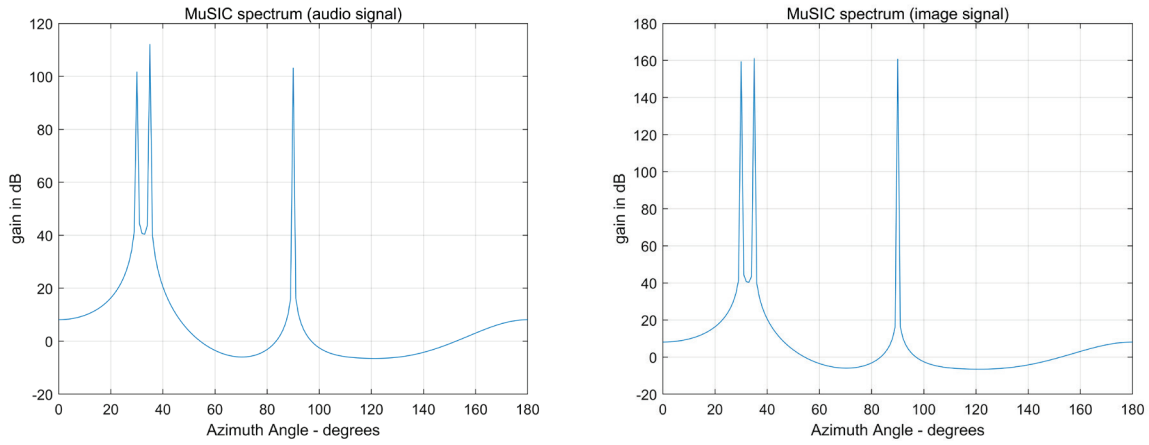

Fig. 3 MuSIC spectrum of the covariance matrix of the audio signal (left) and the image signal (right)

For the uncorrelated sources, the MuSIC algorithm has a high resolution of the DOAs. However, for the coherent sources, the MuSIC algorithm has low performance. For example, when the theoretical covariance is implemented by the $\mathbf{R}_{mm}$ in (13) and the sources from $(30^{\circ}, 0^{\circ})$ and $(35^{\circ}, 0^{\circ})$ are fully correlated, the MuSIC spectrum is shown in Fig. 4. It is noticeable that the sources $(30^{\circ}, 0^{\circ})$ and $(35^{\circ}, 0^{\circ})$ cannot be identified in the spectrum.

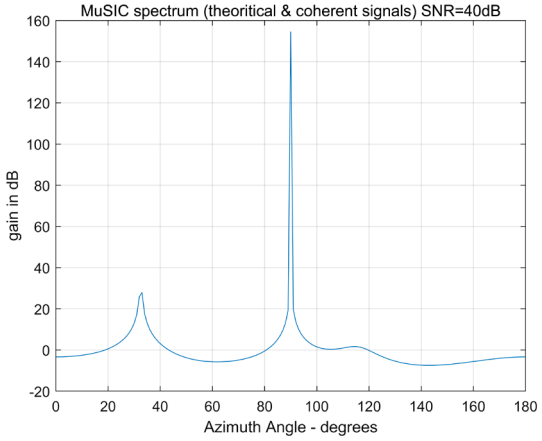

Fig. 4 MuSIC spectrum of the covariance matrix with coherent sources from $(30^{\circ}, 0^{\circ})$ and $(35^{\circ}, 0^{\circ})$.

In order to overcome the coherence problem, a spatial smoothing technique is proposed in [5]. In the smoothing technique, the subarrays with the length K (smaller than the length of the original array) are defined, and the smoothed covariance matrix $\mathbf{R}_{xx,smoothed}$ is used in the MuSIC algorithm instead of the original covariance matrix $\mathbf{R}_{xx}$. The smoothed covariance matrix is defined as

$$\mathbf{R}_{xx,smoothed} = \frac{1}{N}\sum_{s=1}^{N}\mathbf{R}_s \tag{29}$$

where N is the number of subarrays and $\mathbf{R}_s$ is the covariance matrix of the signal received by each subarray. As the length of subarrays is K, both $\mathbf{R}_s$ and $\mathbf{R}_{xx,smoothed}$ are $K \times K$ matrix, which is smaller than the original covariance matrix. It means that the spatial smoothing technique is capable of addressing the coherence problem with the penalty of reducing the aperture of the array. By applying the smoothed covariance matrix, the fully correlated source from $(30^{\circ}, 0^{\circ})$ and $(35^{\circ}, 0^{\circ})$ can be distinguished in the MuSIC spectrum as shown in Fig. 5.

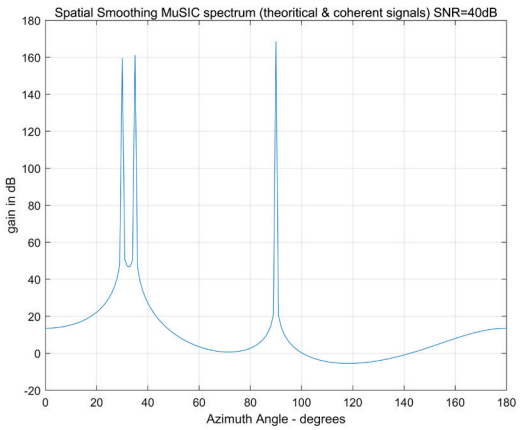

Fig. 5 MuSIC spectrum of the smoothed covariance matrix with coherent sources from $(30^{\circ}, 0^{\circ})$ and $(35^{\circ}, 0^{\circ})$

c) Reception Problem

The objective of the reception problem for array receivers is to receive the desired signals and suppress the remaining unwanted co-channel interference. Beamforming is commonly used in the reception problem at the receiver, which sums the received signal by weights calculated according to the characteristic of the received signal.

One of the conventional beamformers is the Wiener-Hopf beamformer. The DOAs of the three sources in the theoretical covariance matrix and the practical covariance matrices of the audio and the image signal has been estimated using the MuSIC algorithm in the previous section, which are $(30^{\circ}, 0^{\circ})$, $(35^{\circ}, 0^{\circ})$, and $(90^{\circ}, 0^{\circ})$. Assuming the desired source is located at $(90^{\circ}, 0^{\circ})$, the array manifold vector $\underline{S}_{\substack{desired \\ signal}}$ can be calculated as $\underline{S}(90^{\circ}, 0^{\circ})$ using formula (1). The weight of the Wiener-Hopf beamformer is given by

$$\underline{w} = c \cdot \mathbf{R}_{xx}^{-1} \underline{S}_{\substack{desired \\ signal}} \tag{30}$$

where c is a constant scalar and $\mathbf{R}_{xx}^{-1}$ is the inverse of the covariance matrix of the received signal. If the SNR is high (i.e., SNR=40dB), the array pattern with Wiener-Hopf beamformer for the theoretical covariance matrix is shown in Fig. 6 (left), where the sources in the direction of 30° and 35° in suppressed and the gain at the direction 90° is maximized. However, with low SNR (i.e., SNR=10dB), the performance of the Wiener-Hopf beamformer is low. The array pattern (right figure in Fig. 6) is almost the same as the default pattern, which cannot suppress the interference and receive the desired signal.

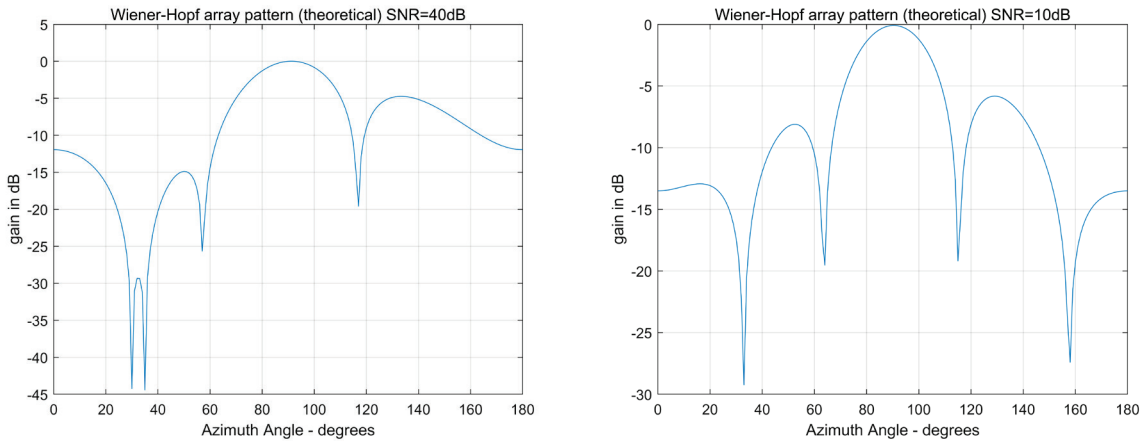

Fig. 6 Array Pattern of the Wiener-Hopf beamformer with SNR=40dB (left) and 10dB (right)

The Wiener-Hopf beamformer is also applied to receive the source from $(90^{\circ}, 0^{\circ})$ in the audio and image signals. The received image is shown in Fig. 7, where there are many interferences. The received audio is also like that there are several sounds overlapped. In the array patterns (Fig. 8) of the Wiener-Hopf beamformer for audio and image signals, interference sources from $(30^{\circ}, 0^{\circ})$ and $(35^{\circ}, 0^{\circ})$ are not suppressed because of the low SNR in the audio and image signals.

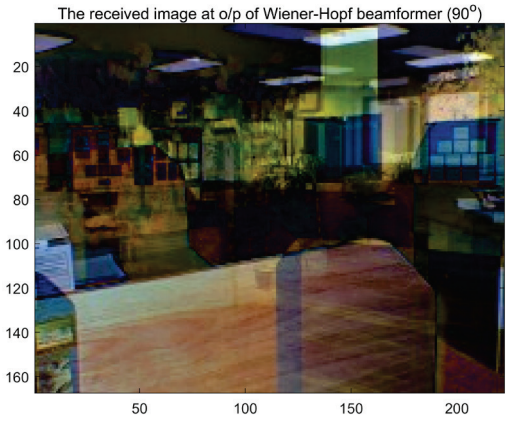

Fig. 7 The image from $(90^{\circ}, 0^{\circ})$ received by the Winer-Hopf beamformer

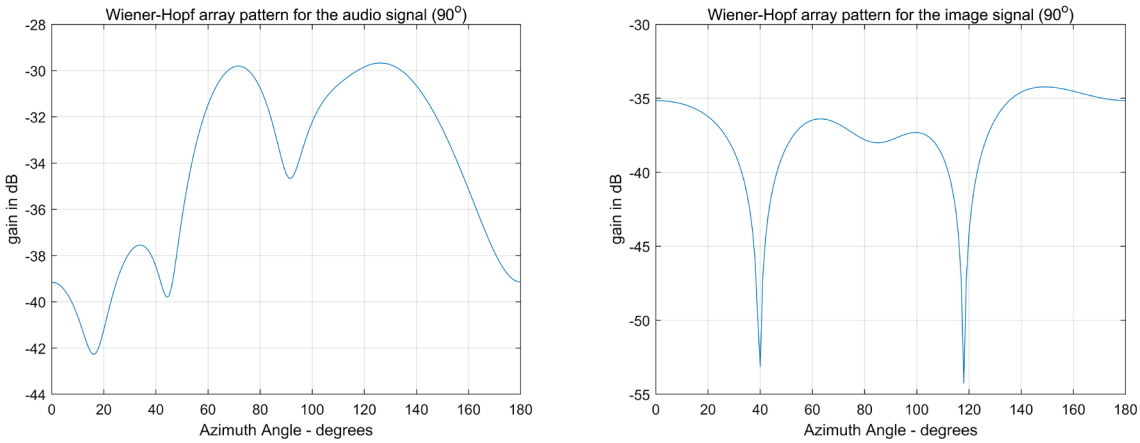

Fig. 8 Array Patterns of the Wiener-Hopf beamformer for audio and image signals to receive the source from 90°

In order to eliminate the impact of the noise on the reception problem, a superresolution beamformer is proposed in [6]. The superresolution beamformer based on the DOA estimation is given by

$$\underline{w} = \mathbb{P}_{\mathbf{S}_J}^{\perp} \underline{S}_{\substack{desired \\ signal}} \tag{31}$$

where $\mathbf{S}_J$ is the matrix consist of the array manifold vectors of the jammers (interference sources). Applying the superresolution beamformer to the image signals, the images from the three sources can be well received, which are shown in Fig. 9, Fig. 10, and Fig. 11. These results indicate that the superresolution beamformer is capable of suppressing the interference signal at low SNR, which eliminates the impact of noise on the resolution.

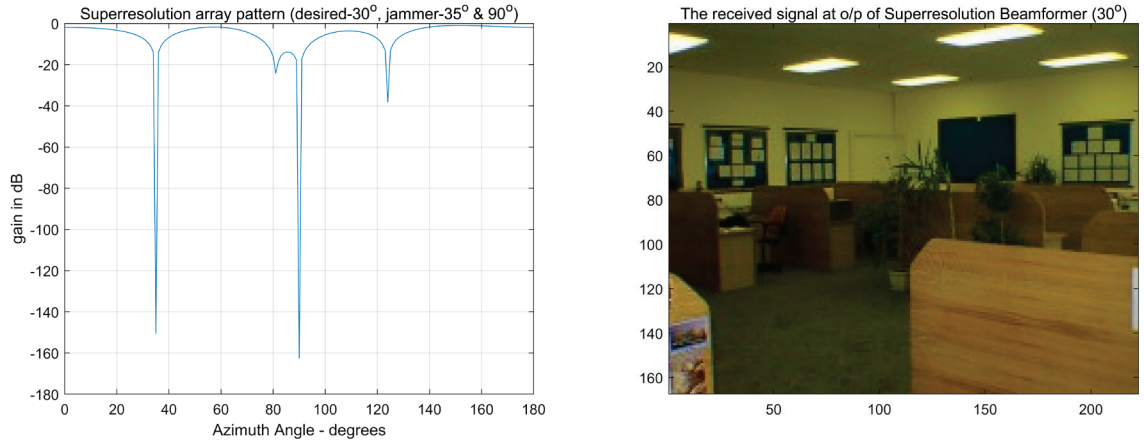

Fig. 9 Array Patterns of the superresolution beamformer for image signals to receive the source from 30° (left) and the received image (right)

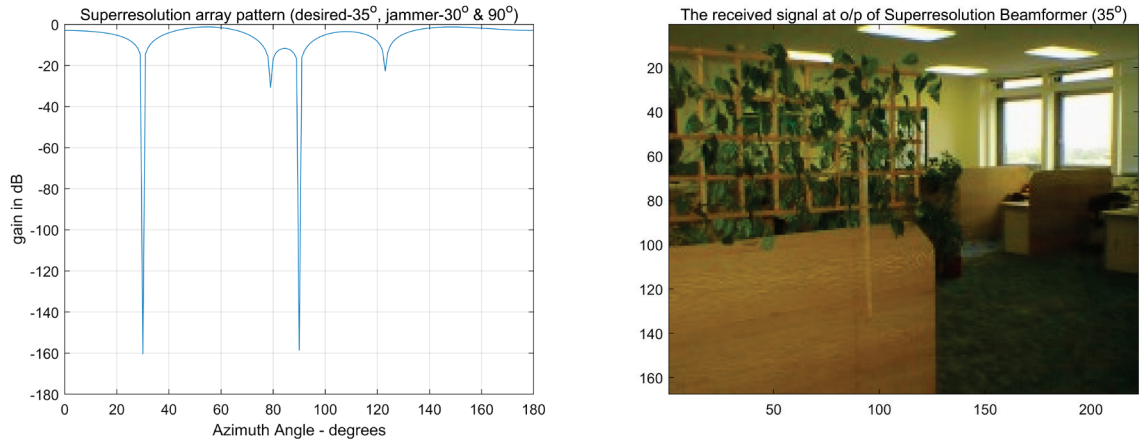

Fig. 10 Array Patterns of the superresolution beamformer for image signals to receive the source from 35° (left) and the received image (right)

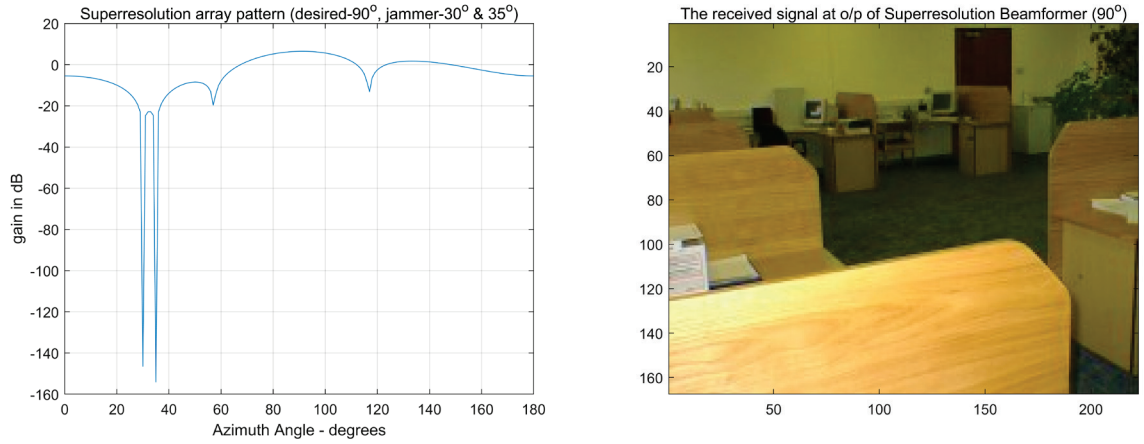

Fig. 11 Array Patterns of the superresolution beamformer for image signals to receive the source from 90° (left) and the received image (right)

IV. CONCLUSION

In the communication system, the desired signal and the interference signals usually arrive at the receiver at the same time and the same frequency band, which leads to the need of suppressing the interference signals. A good solution is to use antennas arrays at the receiver and exploit the array processing and digital communication theory. The covariance matrix of the received signal plays an important role at the array receiver. In the detection problem, the number of emitting sources can be estimated based on the multiplicity of minimum eigenvalues in the covariance matrix in theory, while the AIC and MDL method can be used in practice. The MuSIC algorithm using the array manifold vectors and the noise space of the covariance matrix can be used to estimate the DOAs of the sources in the estimation problem. To receive the desired signal and suppress the interference, the conventional Wiener-Hopf beamformer can be applied, but its performance is subject to the noise. The superresolution beamformer is capable of eliminating the impact of noise on the reception problem and has a great performance even at low SNR.

V. REFERENCES

[1] A. Manikas, “Experiment Handout on Array Communication and Processing”, October. 1998.

[2] M. Wax and T. Kailath, “Detection of signals by information theoretic criteria”, IEEE Transactions on Acoustics, Speech, and Signal Processing, Vol. 33, No. 2, pp. 387-392, April 1985.

[3] R. Schmidt, “Multiple Emitter Location and Signal Parameter Estimation”, IEEE Transactions on Antennas and Propagation, Vol. AP-34, No.3, pp. 276-280, March 1986.

[4] Advanced Communication Theory, A. Manikas. Imperial College London, 2020

[5] T. Shan, M. Wax, T. Kailath, “On Spatial Smoothing for Direction-of-Arrival Estimation of Coherent Signals”, IEEE Transactions on Acoustics, Speech and Signal Processing, Vol. ASSP-33, No.4, pp 806-811, August 1985.

[6] P. D. Karaminas and A. Manikas, “Super-resolution broad null beamforming for cochannel interference cancellation in mobile radio networks”, IEEE Transactions on Vehicular Technology, Vol. 49, No. 3, pp. 689-697, May 2000